

Supporting Information for:

Selective Adsorption of Ethylene over Ethane and Propylene over Propane in the Metal-Organic Frameworks $M_2(\text{dobdc})$ ($M = \text{Mg}, \text{Mn}, \text{Fe}, \text{Co}, \text{Ni}, \text{Zn}$)

Stephen J. Geier,^a Jarad A. Mason,^a Eric D. Bloch,^a
Wendy L. Queen,^{b,c} Matthew R. Hudson,^c Craig M. Brown,^{c,d}
Jeffrey R. Long^{*a,e}

^aDepartment of Chemistry, University of California, Berkeley, CA 94720, USA; E-mail: jrlong@berkeley.edu;

^bThe Molecular Foundry, Lawrence Berkeley National Laboratory, Berkeley, CA 94720, USA

^cCenter for Neutron Research, National Institute of Standards and Technology, Gaithersburg, MD 20899, USA

^dDepartment of Chemical Engineering, University of Delaware, Newark, DE 19716, USA

^eMaterials Sciences Division, Lawrence Berkeley National Laboratory, Berkeley, CA 94720, USA

Chem. Sci.

List of Contents

1. Sample Preparation and Activation	S-3
2. Gas Adsorption Measurements	S-3
3. Fitting of Isotherms.....	S-6
4. Dual-site Langmuir-Freundlich Fits	S-7
Mg ₂ (dobdc).....	S-7
Mn ₂ (dobdc)	S-9
Co ₂ (dobdc).....	S-11
Ni ₂ (dobdc)	S-13
Zn ₂ (dobdc).....	S-15
Fe ₂ (dobdc)	S-17
5. Gravimetric and Volumetric Capacities.....	S-18
6. Isosteric Heats of Adsorption.....	S-18
7. IAST Selectivity Calculations	S-20
8. Neutron Powder Diffraction	S-21
9. Comparison to Prior Studies.....	S-28
10. References.....	S-31

1. Sample Preparation and Activation

All reagents were obtained from commercial vendors[#] and used without further purification. $Mg_2(dobdc)$,¹ $Fe_2(dobdc)$,² $Co_2(dobdc)$,¹ $Ni_2(dobdc)$ ¹ and $Zn_2(dobdc)$ ¹ were synthesized according to previously published methods. $Mn_2(dobdc)$ was prepared by mixing 2,5-dihydroxyterephthalic acid (30 mg, 0.15 mmol) with $MnCl_2$ (47 mg, 38 mmol, 2.5 eq.) in 3 mL of anhydrous methanol and 17 mL of anhydrous N,N-dimethylformamide in a 20 mL vial under an inert atmosphere. The solution was heated in a Teflon-capped vial at 120 °C for 18 hours. All as-synthesized materials were subjected to two hot (100-120 °C) DMF washes, followed by exchanging with hot MeOH (70 °C, 5 exchange cycles of 6-12 hours). MeOH-solvated materials were activated for 24 hours at 180 °C. Powder diffraction patterns are consistent with those reported previously. Langmuir surface areas and calculated pore volumes are consistent with or greater than those previously reported (Fig. S1 and Table S1).

2. Gas Adsorption Measurements

Gas adsorption experiments were performed for each gas (ethane, ethylene, propane, propylene and acetylene) at 318 K, 333 K and 353 K on each $M_2(dobdc)$. For all gas adsorption measurements, MeOH-solvated $M_2(dobdc)$ was transferred to a pre-weighed glass sample tube under an atmosphere of nitrogen and capped with a Transeal. Samples were then transferred to a Micromeritics ASAP 2020 gas adsorption analyzer and heated at a rate of 0.1 K/min from room

[#]Certain commercial materials and equipment are identified in this paper only to specify adequately the experimental procedure and in no case does such identification imply recommendation by NIST nor does it imply that the material/equipment identified is necessarily the best for this purpose.

temperature to a final temperature of 453 K. Samples were considered fully activated when the outgas rate at 453 K was less than 2 μ bar/min. Evacuated tubes containing degassed samples were then transferred to a balance and weighed to determine the mass of sample, typically 90–175 mg. The tube was transferred to the analysis port of the instrument where the outgas rate was again confirmed to be less than 2 μ bar/min at 433 K. Langmuir surface areas and pore volumes were determined by measuring N₂ adsorption isotherms in a 77 K liquid nitrogen bath and calculated using the Micromeritics software. All other adsorption measurements were performed using a recirculating dewar (Micromeritics) connected to a Julabo F32-MC isothermal bath. UHP-grade (99.999% purity) nitrogen and helium were used for all adsorption measurements. For ethane, ethylene, propane, and propylene adsorption, 99.99% or higher purity gases were used. After each isotherm measurement, the sample was evacuated under dynamic vacuum, until the outgas rate was less than 2 μ bar/min, prior to continuing on to the next measurement.

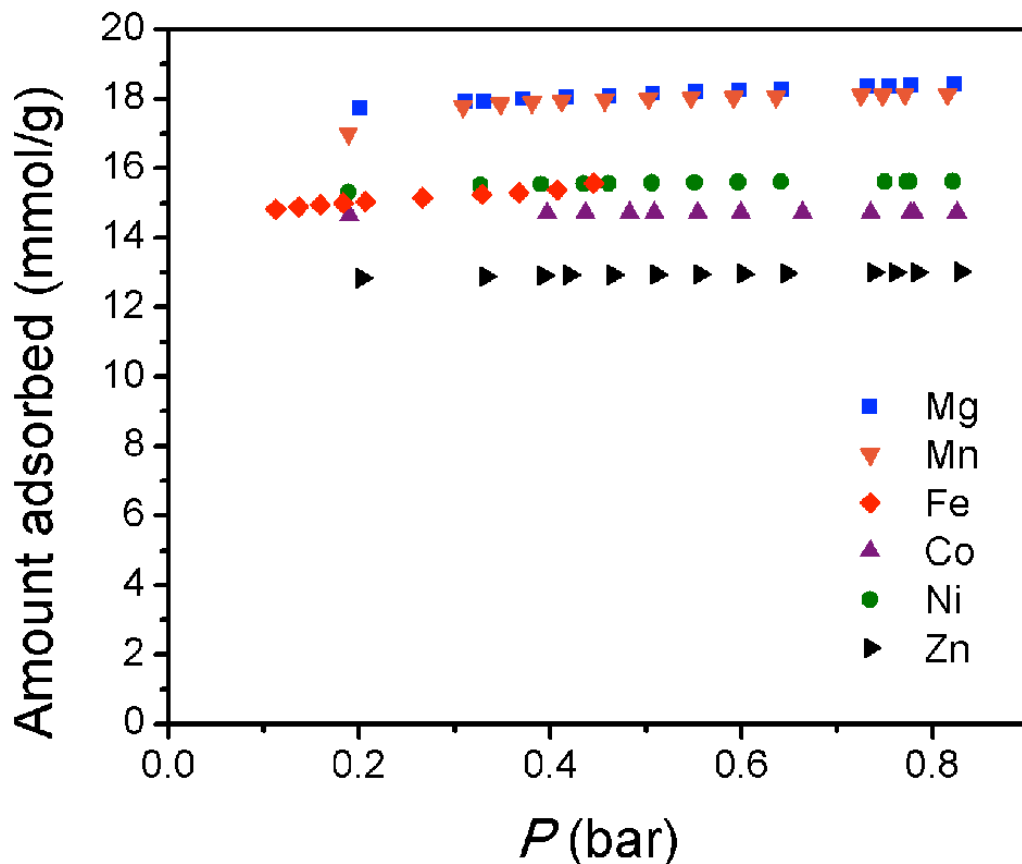


Fig. S1 Saturation N₂ uptake at 77 K for M₂(dobdc) (M = Mg, Mn, Fe, Co, Ni, Zn) used to calculate Langmuir surface areas and pore volumes. Note that the data for Fe₂(dobdc) is taken from Ref. 4.

Table S1 Langmuir surfaces areas and pore volumes for M₂(dobdc).

M ₂ (dobdc)	Langmuir Surface Area (m ² /g)	Calculated Pore Volume (cm ³ /g)
Mg	1835	0.638
Mn	1797	0.628
Fe	1536	0.529
Co	1438	0.510
Ni	1532	0.541
Zn	1277	0.451

3. Fitting of Isotherms

The experimentally measured excess adsorption isotherms of all hydrocarbons were first converted to absolute loadings by using the following procedure. The fluid densities at each temperature were determined using the NIST Thermochemical Properties of Fluid Systems.³ Subsequently, these values were multiplied by the pore volume of each material (Table S1) to obtain the amount of gas that would be present in the pore space in the absence of adsorption. The absolute loadings were determined by adding these values to the experimentally measured excess loadings. All isotherm fits, and subsequent analyses to determine selectivities and isosteric heats of adsorption, were carried out using absolute loadings.

The absolute adsorption isotherms were fit with a dual-site Langmuir-Freundlich model (Eqn 1), where n is the absolute amount adsorbed in mmol/g, P is the pressure in bar, $q_{\text{sat},i}$ is the saturation capacity in mmol/g, b_i is the Langmuir parameter in bar⁻¹, and v_i is the Freundlich parameter for two sites 1 and 2. The fitted parameters for each adsorption isotherm can be found in Tables S2-S11. Plots of the absolute adsorption isotherms with the corresponding dual-site Langmuir-Freundlich fits can be found in Fig. S2-S6. Note that the pure component isotherms and dual-site Langmuir-Freundlich parameters for Fe₂(dobdc) have been recently published and all values in this work were taken as previously reported.⁴

$$n = \frac{q_{\text{sat},1}b_1P^{v_1}}{1+b_1P^{v_1}} + \frac{q_{\text{sat},2}b_2P^{v_2}}{1+b_2P^{v_2}} \quad (1)$$

4. Dual-site Langmuir-Freundlich Fits

Mg₂(dobdc)

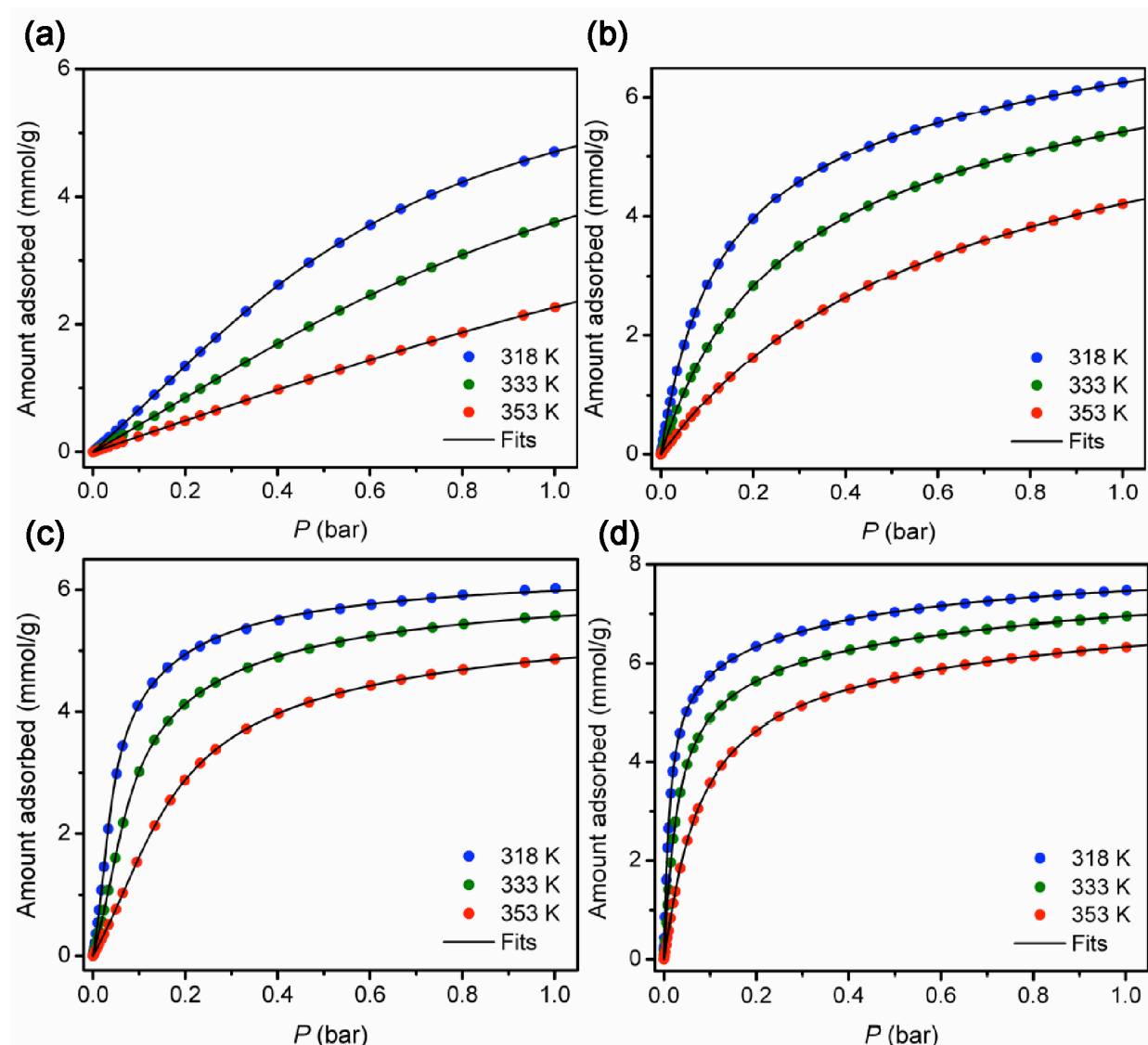


Fig. S2 Pure component isotherm data for ethane (a), ethylene (b), propane (c) and propylene (d) in $\text{Mg}_2(\text{dobdc})$. The black lines are the respective dual-site Langmuir-Freundlich fits using the parameters in Table S2 and S3.

Table S2 Dual-site Langmuir-Freundlich parameters for pure ethane and ethylene adsorption isotherms in Mg₂(dobdc).

Mg ₂ (dobdc)	Ethane			Ethylene		
	318 K	333 K	353 K	318 K	333 K	353 K
qsat1	5.6	5.5	5	2	1.9	1.9
b1	2.34	1.11	0.58	0.54	0.212	0.095
v1	1.61	1.58	1.52	1.5	1.64	1.1
qsat2	0.89	0.9	0.91	6.2	6.4	6.5
b2	6.9	4.2	2.34	8.27	3.88	1.63
v2	1	1	1	1	1	1

Table S3 Dual-site Langmuir-Freundlich parameters for pure propane and propylene adsorption isotherms in Mg₂(dobdc).

Mg ₂ (dobdc)	Propane			Propylene		
	318 K	333 K	353 K	318 K	333 K	353 K
qsat1	1.69	1.63	1.77	5.59	5.51	5.67
b1	12167	1088	78.7	166.5	65.6	20.6
v1	2.81	2.58	2.24	1.14	1.15	1.13
qsat2	4.66	4.51	3.95	2.57	2.39	2.26
b2	11.7	6.67	3.68	2.89	1.76	0.7
v2	1	1	1	1	1	1

Mn₂(dobdc)

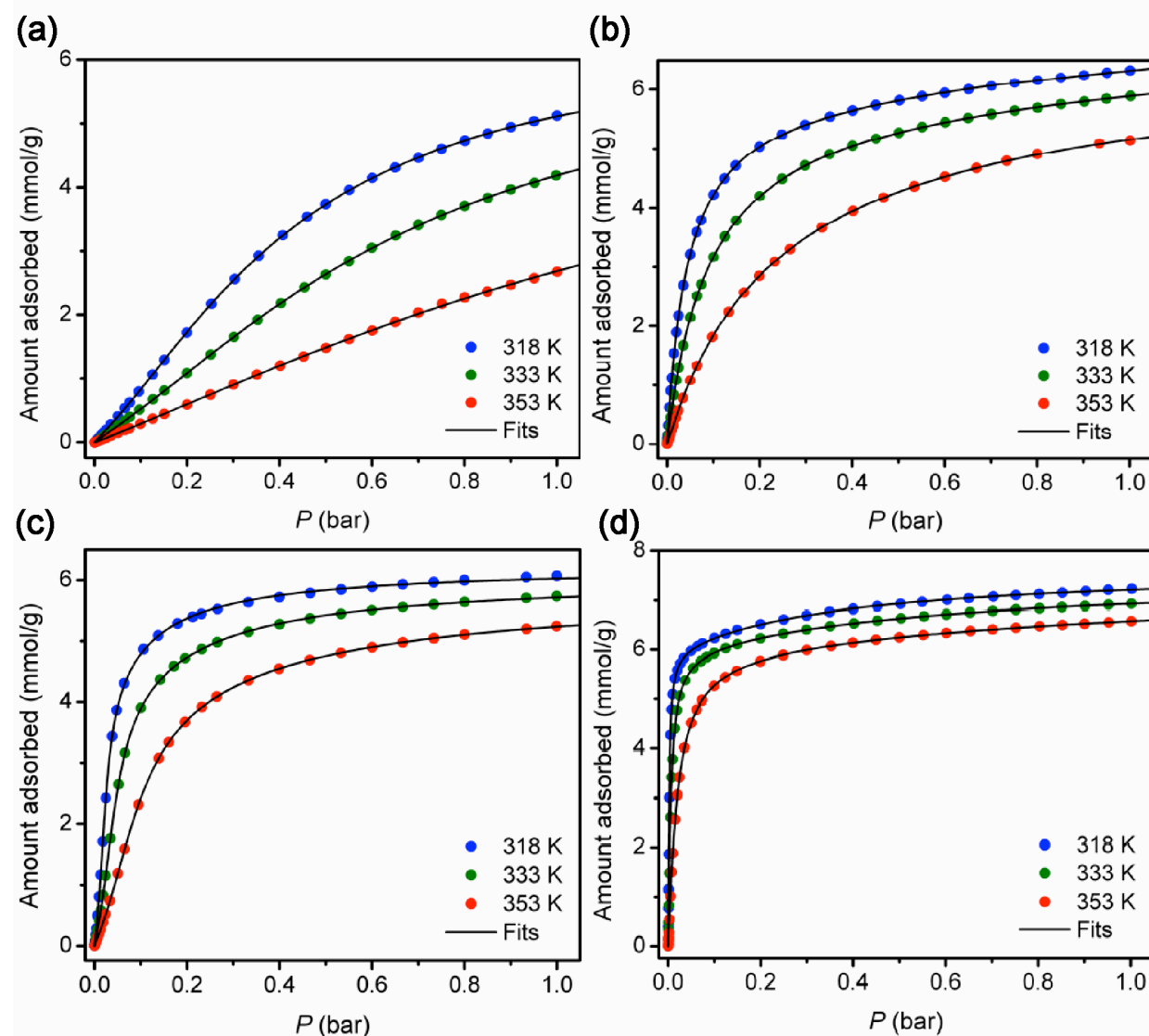


Fig. S3 Pure component isotherm data for ethane (a), ethylene (b), propane (c) and propylene (d) in $\text{Mn}_2(\text{dobdc})$. The black lines are the respective dual-site Langmuir-Freundlich fits using the parameters in Table S4 and S5.

Table S4 Dual-site Langmuir-Freundlich parameters for pure ethane and ethylene adsorption isotherms in Mn₂(dobdc).

Mn₂(dobdc)	Ethane			Ethylene		
	<i>318 K</i>	<i>333 K</i>	<i>353 K</i>	<i>318 K</i>	<i>333 K</i>	<i>353 K</i>
qsat1	5.84	5.71	5.71	3.11	2.99	2.93
b1	3.81	1.84	0.65	0.24	0.16	0.057
v1	1.58	1.56	1.4	1.08	1.03	1.01
qsat2	0.52	0.54	0.54	5.97	5.98	6.19
b2	13.4	8.46	3.83	23	11	4.19
v2	1	1	1	1	1	1

Table S5 Dual-site Langmuir-Freundlich parameters for pure propane and propylene adsorption isotherms in Mn₂(dobdc).

Mn₂(dobdc)	Propane			Propylene		
	<i>318 K</i>	<i>333 K</i>	<i>353 K</i>	<i>318 K</i>	<i>333 K</i>	<i>353 K</i>
qsat1	2.21	2.08	1.93	5.89	5.88	5.93
b1	47375	3841	353.9	1836	453.8	96.2
v1	2.87	2.66	2.46	1.24	1.19	1.16
qsat2	4.02	4	3.94	1.81	1.66	1.71
b2	18.5	10.3	5.2	2.76	1.78	0.72
v2	1	1	1	1	1	1

Co₂(dobdc)

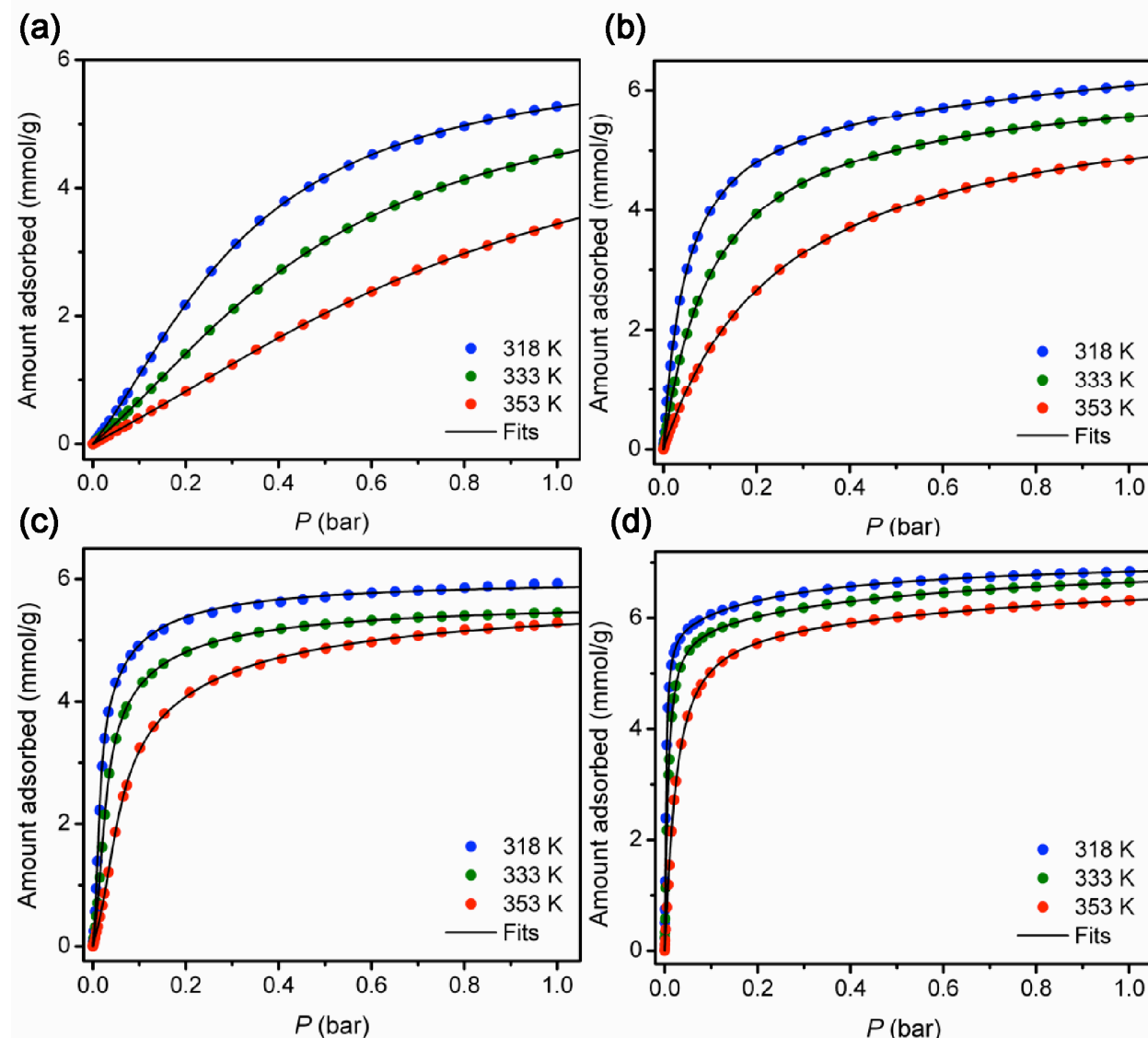


Fig. S4 Pure component isotherm data for ethane (a), ethylene (b), propane (c) and propylene (d) in *Co₂(dobdc)*. The black lines are the respective dual-site Langmuir-Freudlich fits using the parameters in Table S6 and S7.

Table S6 Dual-site Langmuir-Freundlich parameters for pure ethane and ethylene adsorption isotherms in Co₂(dobdc).

Co ₂ (dobdc)	Ethane			Ethylene		
	318 K	333 K	353 K	318 K	333 K	353 K
qsat1	5.69	5.46	5.36	2.98	2.87	2.68
b1	5.87	3.1	1.32	0.21	0.059	0.013
v1	1.55	1.56	1.52	1.11	1.05	1
qsat2	0.41	0.42	0.43	5.81	5.97	6.07
b2	20.9	14.4	8.24	20.9	9.47	3.87
v2	1	1	1	1	1	1

Table S7 Dual-site Langmuir-Freundlich parameters for pure propane and propylene adsorption isotherms in Co₂(dobdc).

Co ₂ (dobdc)	Propane			Propylene		
	318 K	333 K	353 K	318 K	333 K	353 K
qsat1	2.05	1.94	1.69	5.69	5.67	5.67
b1	586270	29985	3530	2450	594	115
v1	3.08	2.79	2.75	1.35	1.29	1.24
qsat2	3.96	3.71	4.04	1.43	1.45	1.47
b2	26.6	17	7.56	4.15	2.09	0.909
v2	1	1	1	1	1	1

Ni₂(dobdc)

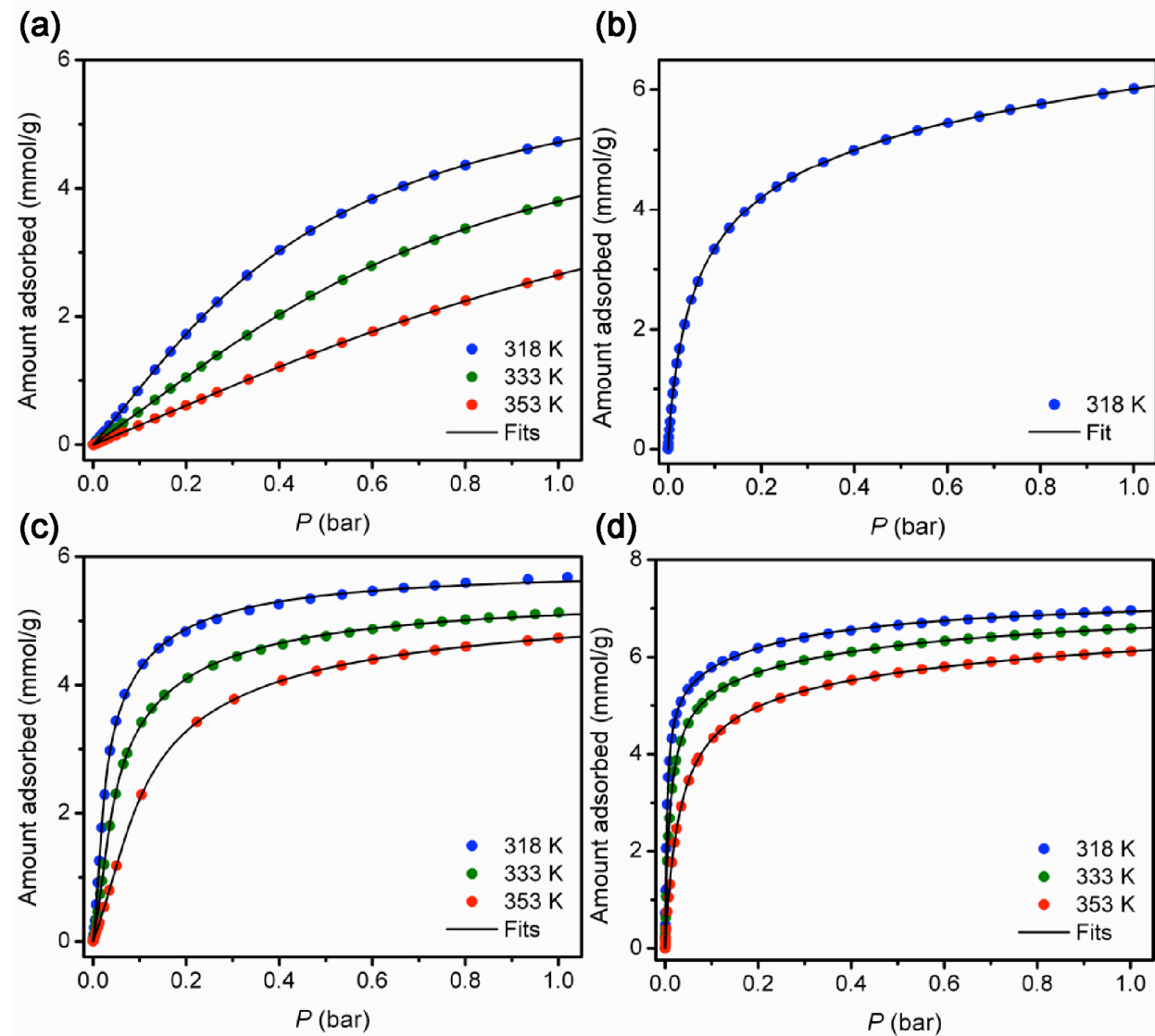


Fig. S5 Pure component isotherm data for ethane (a), ethylene (b), propane (c) and propylene (d) in Ni₂(dobdc). The black lines are the respective dual-site Langmuir-Freundlich fits using the parameters in Table S8 and S9.

Table S8 Dual-site Langmuir-Freundlich parameters for pure ethane and ethylene adsorption isotherms in Ni₂(dobdc).

Ni ₂ (dobdc)	Ethane			Ethylene		
	318 K	333 K	353 K	318 K	333 K	353 K
qsat1	5.66	5.4	5.42	5.2	-	-
b1	3.28	1.74	0.74	11.6	-	-
v1	1.42	1.45	1.38	0.87	-	-
qsat2	0.4	0.4	0.4	3.3	-	-
b2	17.	10.7	5.42	0.58	-	-
v2	1	1	1	1	-	-

Table S9 Dual-site Langmuir-Freundlich parameters for pure propane and propylene adsorption isotherms in Ni₂(dobdc).

Ni ₂ (dobdc)	Propane			Propylene		
	318 K	333 K	353 K	318 K	333 K	353 K
qsat1	1.44	1.18	1.33	5.26	5.38	5.34
b1	47463	8313	327.9	387.5	93.1	35.6
v1	2.71	2.69	2.34	1.08	0.98	1.02
qsat2	4.40	4.27	4.03	2.04	1.81	1.8
b2	17.7	10.9	5.46	4.81	2.3	1.04
v2	1	1	1	1	1	1

Zn₂(dobdc)

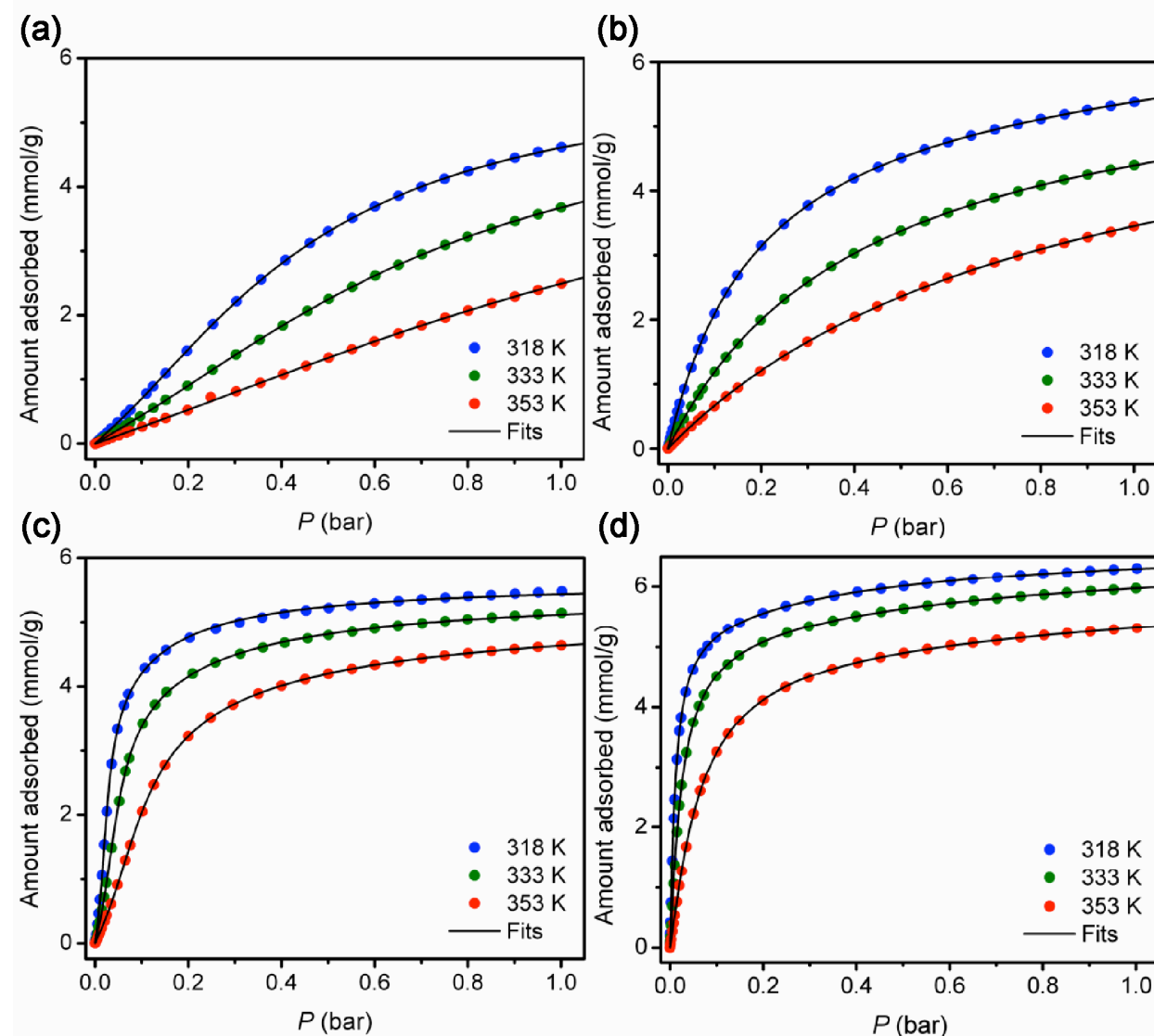


Fig. S6 Pure component isotherm data for ethane (a), ethylene (b), propane (c) and propylene (d) in Zn₂(dobdc). The black lines are the respective dual-site Langmuir-Freundlich fits using the parameters in Table S10 and S11.

Table S10 Dual-site Langmuir-Freundlich parameters for pure ethane and ethylene adsorption isotherms in Zn₂(dobdc).

Zn ₂ (dobdc)	Ethane			Ethylene		
	318 K	333 K	353 K	318 K	333 K	353 K
qsat1	5.12	5.1	5.09	6	6	6
b1	3.75	1.66	0.64	0.03	0.0027	0.0077
v1	1.66	1.6	1.53	2.04	2.2	0.97
qsat2	0.62	0.56	0.67	6.24	6.23	6.31
b2	10.3	7.32	3.34	5.04	2.36	1.17
v2	1	1	1	1	1	1

Table S11 Dual-site Langmuir-Freundlich parameters for pure propane and propylene adsorption isotherms in Zn₂(dobdc).

Zn ₂ (dobdc)	Propane			Propylene		
	318 K	333 K	353 K	318 K	333 K	353 K
qsat1	1.93	1.8	1.77	5.21	5.09	5.02
b1	70280	5163	325	209	86.8	25.7
v1	3.02	2.78	2.5	1.18	1.19	1.17
qsat2	3.73	3.67	3.45	1.59	1.57	1.71
b2	16.3	9.24	4.94	2.35	1.49	0.40
v2	1	1	1	1	1	1

Fe₂(dobdc)

Table S12 Dual-site Langmuir-Freundlich parameters for pure ethane and ethylene adsorption isotherms in Fe₂(dobdc). Reproduced from Ref. 4.

Fe₂(dobdc)	Ethane			Ethylene		
	318 K	333 K	353 K	318 K	333 K	353 K
qsat1	5	5	5	3.6	3.6	3.6
b1	5.4	2.2	0.8	117.3	40.5	33.3
v1	1.7	1.6	1.5	1.1	1.1	1.01
qsat2	1	1	1	3.3	3.3	3.3
b2	7.9	4.4	2.7	8.3	4.9	9.8
v2	1	1	1	1	1	1

Table S13 Dual-site Langmuir-Freundlich parameters for pure propane and propylene adsorption isotherms in Fe₂(dobdc). Reproduced from Ref. 4.

Fe₂(dobdc)	Propane			Propylene		
	318 K	333 K	353 K	318 K	333 K	353 K
qsat1	2.4	2.2	2.2	5.2	6	5.9
b1	71843	4914	208	9694	822	156
v1	2.85	2.53	2.08	1.42	1.26	1.2
qsat2	3.9	3.9	3.6	1.8	1.4	1.1
b2	19.3	11.3	5.7	12.1	2.06	2.01
v2	1	1	1	1	1	1

5. Gravimetric and Volumetric Capacities

Table S14 Gravimetric ethylene and propylene capacities for M₂(dobdc) at 1 bar and 318 K.

M ₂ (dobdc)	Ethylene capacity (mmol/g)	Propylene capacity (mmol/g)
Mg	6.24	7.49
Mn	6.33	7.23
Fe	6.30	6.90
Co	6.07	6.84
Ni	6.01	6.96
Zn	5.38	6.31

Table S15 Volumetric ethylene and propylene capacities for M₂(dobdc) at 1 bar and 318 K.

M ₂ (dobdc)	Crystallographic Density (g/cm ³)	Ethylene capacity (mmol/cm ³)	Propylene capacity (mmol/cm ³)
Mg	0.909	5.67	6.80
Mn	1.084	6.86	7.84
Fe	1.126	7.09	7.77
Co	1.169	7.10	8.00
Ni	1.206	7.25	8.39
Zn	1.231	6.62	7.76

6. Isosteric Heats of Adsorption

The Clausius-Clapeyron equation (Eqn 2) was used to calculate the isosteric heats of adsorption, -Q_{st}, for each hydrocarbon and M₂(dobdc) analogue, using the dual-site Langmuir-Freundlich fits for each material at 318 K, 333 K, and 353 K.

$$\ln P = -\frac{Q_{st}}{R} \left(\frac{1}{T} \right) + C \quad (2)$$

Here, *P* is the pressure, *n* is the amount adsorbed, *T* is the temperature, R is the universal gas constant, and C is a constant. The isosteric heat of adsorption, -Q_{st}, was obtained from the slope

of plots of $(\ln P)_n$ as a function of $1/T$. The isosteric heats of adsorption as a function of loading for each hydrocarbon in $M_2(\text{dobdc})$ can be found in Figure S7.

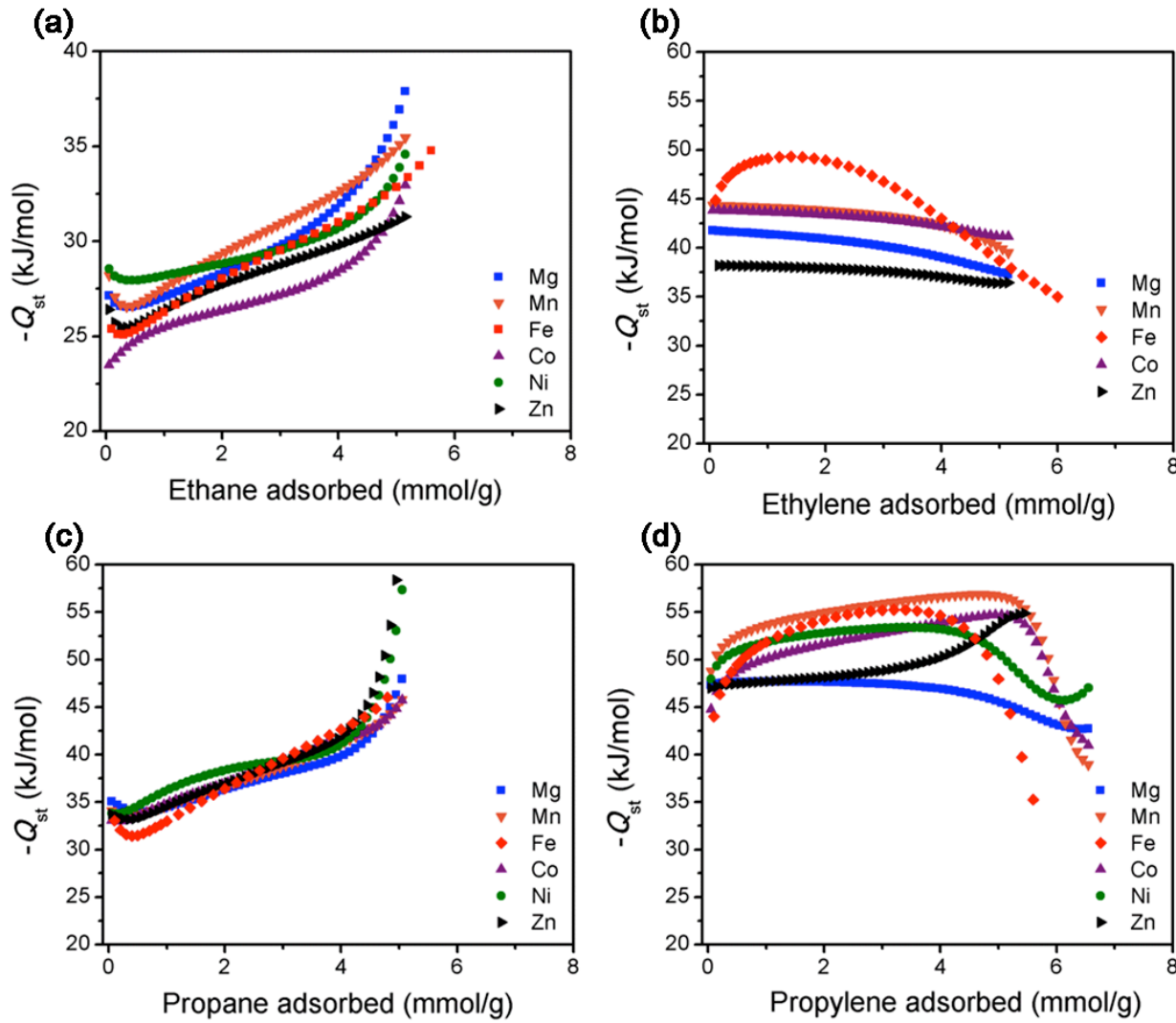


Fig. S7 Isosteric heats of adsorption as a function of amount adsorbed for ethane (a), ethylene (b), propane (c), and propylene (d) in $M_2(\text{dobdc})$.

7. IAST Selectivity Calculations

In order to determine the selectivity factor, S_{ads} , for binary mixtures using pure component isotherm data, it is necessary to use an adsorption model, such as ideal adsorbed solution theory (IAST).⁵

The IAST estimations of adsorption selectivities were calculated for propylene/propane and ethylene/ethane mixtures of varying compositions (5:95 to 95:5) at 313 K and a total pressure of 1 bar. Note that the selectivity factor, S , is defined according to Equation 3 where n is the amount of each component adsorbed as determined from IAST and x is the mole fraction of each component in the gas phase at equilibrium. The IAST selectivity factors for a 50:50 mixture of alkene:alkane can be found in Table S16.

$$S = \frac{n_{\text{alkene}}/n_{\text{alkane}}}{x_{\text{alkene}}/x_{\text{alkane}}} \quad (3)$$

Table S16 IAST selectivities for an equimolar alkene/alkane mixtures at 1 bar, 318 K.

M ₂ (dobdc)	Ethylene/Ethane Selectivity	Propylene/Propane Selectivity
Mg	4.44	5.55
Mn	8.13	16.6
Fe	13.6	14.7
Co	5.82	8.63
Ni	5.93	10.4
Zn	2.70	3.89

8. Neutron Powder Diffraction

Neutron powder diffraction (NPD) experiments were carried out on 0.9702 g and 0.8650 g of activated $\text{Co}_2(\text{dobdc})$ and $\text{Mn}_2(\text{dobdc})$ using the high-resolution neutron powder diffractometer, BT1, at the National Institute of Standards and Technology Center for Neutron Research (NCNR). The sample was placed in a He purged glove box, loaded into a vanadium can equipped with a gas loading valve, and sealed using an In O-ring. NPD data were collected using a Ge(311) monochromator with an in-pile 60° collimator corresponding to a wavelength of 2.0782 Å. The sample was loaded onto a bottom-loading closed cycle refrigerator and data were collected on the bare framework at 10 K. For gas loading, the sample was warmed to 300 K and then exposed to a predetermined amount of gas. Upon reaching an equilibrium pressure at the loading temperature, the sample was then slowly cooled to ensure equilibrium and complete adsorption of the hydrocarbon. Data were collected at 10 K for loadings of 0.5 ethane or ethylene molecules per metal and loadings that range from 0.25 to 0.33 propylene molecules per metal for $\text{Mn}_2(\text{dobdc})$ and $\text{Co}_2(\text{dobdc})$, respectively (Table S17). Between loadings the samples were allowed to slowly warm to room temperature while under dynamic vacuum. The samples remained under vacuum with slight heating in order to fully outgas the frameworks before subsequent gas loading measurements were carried out. Rietveld refinements were carried out using the EXPGUI package.¹⁰

Table S17 Summary of gas dosing amounts for neutron powder diffraction experiments.

$\text{M}_2(\text{dobdc})$	Gas	Loading in mmol/g (molecules per M)
Mn	C_2D_6	3.29 (0.5)
Mn	C_2D_4	3.29 (0.5)
Mn	C_3D_6	2.0 (0.3)
Co	C_2D_6	3.2 (0.5)
Co	C_2D_4	3.2 (0.5)
Co	C_3D_6	1.6 (0.25)

Table S18 Crystallographic data for activated Co₂(dobdc), space group R-3, $a = 25.9067(9)$ Å, $c = 6.8548(5)$ Å, $V = 3984.3(3)$ Å³, goodness of fit parameters, Rp = 0.0316, wRp = 0.0379, $\chi^2 = 1.029$. Values in parentheses indicate one standard deviation in the refined value.

Atom	X	Y	Z	Occ	Uiso (Å ²)	Multiplicity
Co	0.384(1)	0.349(1)	0.136(4)	1.0	0.003(7)	18
O1	0.3283(6)	0.2968(6)	0.367(2)	1.0	0.018(3)	18
O2	0.3011(6)	0.2279(6)	0.603(2)	1.0	0.001(3)	18
O3	0.3547(6)	0.2749(6)	0.011(2)	1.0	0.000(3)	18
C1	0.3160(6)	0.2470(6)	0.424(2)	1.0	0.029(4)	18
C2	0.3290(6)	0.2075(5)	0.288(2)	1.0	0.020(4)	18
C3	0.3477(6)	0.2257(7)	0.089(2)	1.0	0.028(4)	18
C4	0.3503(6)	0.1810(5)	-0.026(2)	1.0	0.008(3)	18
H1	0.3647(9)	0.1951(7)	-0.175(3)	1.0	0.001(4)	18

Table S19 Crystallographic data for Co₂(dobdc) loaded with 0.5 C₂D₆ per Co(II), space group R-3. $a = 25.919(1)$ Å, $c = 6.8427(4)$ Å, $V = 3981.0(3)$ Å³, goodness of fit parameters, Rp = 0.0261, wRp = 0.0347, $\chi^2 = 0.8673$. Values in parentheses indicate one standard deviation in the refined value.

Atom	X	Y	Z	Occ	Uiso (Å ²)	Multiplicity
Co	0.383(1)	0.349(1)	0.136(4)	1.0	0.010(9)	18
O1	0.3257(6)	0.2967(5)	0.368(2)	1.0	0.010(3)	18
O2	0.3015(5)	0.2298(6)	0.603(2)	1.0	0.004(3)	18
O3	0.3537(5)	0.2722(6)	0.010(2)	1.0	0.0063(3)	18
C1	0.3166(5)	0.2465(5)	0.427(2)	1.0	0.014(3)	18
C2	0.3278(6)	0.2064(6)	0.293(2)	1.0	0.032(3)	18
C3	0.3453(5)	0.2229(5)	0.089(2)	1.0	0.012(2)	18
C4	0.3515(5)	0.1810(6)	-0.028(2)	1.0	0.015(3)	18
H1	0.3630(9)	0.1935(8)	-0.173(4)	1.0	0.015(6)	18
C1a	0.529(1)	0.851(1)	0.647(4)	0.496(7)	0.030(9)	18
C2a	0.510(2)	0.856(2)	0.854(7)	0.496(7)	0.10(1)	18
D3	0.501(2)	0.809(2)	0.590(5)	0.496(7)	0.07(2)	18
D4	0.526(2)	0.881(1)	0.551(4)	0.496(7)	0.05(1)	18
D5	0.573(2)	0.861(2)	0.638(6)	0.496(7)	0.08(1)	18
D6	0.542(1)	0.900(1)	0.913(4)	0.496(7)	0.046(9)	18
D7	0.468(2)	0.854(2)	0.842(7)	0.496(7)	0.09(1)	18
D8	0.507(2)	0.822(2)	0.945(5)	0.496(7)	0.08(1)	18

Table S20 Crystallographic data for Co₂(dobdc) loaded with 0.5 C₂D₄ per Co(II), space group R-3, $a = 25.8741(7)$ Å, $c = 6.8922(3)$ Å, $V = 3996.0(2)$ Å³, goodness of fit parameters, Rp = 0.0186, wRp = 0.0250, $\chi^2 = 1.120$. Values in parentheses indicate one standard deviation in the refined value.

Atom	X	Y	Z	Occ	Uiso (Å ²)	Multiplicity
Co	0.385(1)	0.352(1)	0.144(3)	1.0	0.007(6)	18
O1	0.3225(4)	0.2947(4)	0.364(2)	1.0	0.011(3)	18
O2	0.3028(4)	0.2268(4)	0.599(1)	1.0	0.003(3)	18
O3	0.3525(6)	0.2742(5)	0.002(1)	1.0	0.015(3)	18
C1	0.3155(4)	0.2482(4)	0.419(1)	1.0	0.029(3)	18
C2	0.3300(4)	0.2069(4)	0.287(1)	1.0	0.031(3)	18
C3	0.3478(4)	0.2263(4)	0.085(1)	1.0	0.016(2)	18
C4	0.3523(4)	0.1825(4)	-0.027(1)	1.0	0.016(3)	18
H1	0.3593(8)	0.1890(7)	-0.166(3)	1.0	0.019(4)	18
C11	0.968(1)	0.7911(9)	0.875(3)	0.546(6)	0.035(7)	18
C12	1.0007(8)	0.7929(7)	1.012(2)	0.546(6)	0.021(5)	18
D1a	0.9216(8)	0.7674(8)	0.874(3)	0.546(6)	0.027(7)	18
D2b	1.048(1)	0.824(1)	1.008(4)	0.546(6)	0.057(8)	18
D2a	0.9831(8)	0.7753(9)	1.151(3)	0.546(6)	0.026(5)	18
D1b	0.9872(9)	0.8144(9)	0.751(2)	0.546(6)	0.036(7)	18

Table S21 Crystallographic data for Co₂(dobdc) loaded with 0.3 C₃D₆ per Co(II), space group R-3, $a = 25.8771(8)$ Å, $c = 6.8839(4)$ Å, $V = 3992.1(2)$ Å³, goodness of fit parameters, Rp = 0.0217, wRp = 0.0268, $\chi^2 = 1.204$. Values in parentheses indicate one standard deviation in the refined value.

Atom	X	Y	Z	Occ	Uiso (Å ²)	Multiplicity
Co	0.383(1)	0.352(1)	0.138(4)	1.0	0.000(6)	18
O1	0.3268(5)	0.2991(5)	0.365(2)	1.0	0.005(3)	18
O2	0.3026(6)	0.2284(5)	0.602(2)	1.0	0.001(3)	18
O3	0.3535(6)	0.2737(6)	0.003(2)	1.0	0.007(3)	18
C1	0.3164(5)	0.2444(5)	0.418(2)	1.0	0.023(4)	18
C2	0.3296(6)	0.2062(6)	0.289(2)	1.0	0.030(4)	18
C3	0.3469(6)	0.2245(6)	0.093(2)	1.0	0.035(4)	18
C4	0.3504(5)	0.1816(5)	-0.032(1)	1.0	0.007(3)	18
H	0.361(1)	0.190(1)	-0.179(4)	1.0	0.043(6)	18
C11	0.972(2)	0.797(1)	0.846(5)	0.363(6)	0.009(8)	18
C12	1.001(2)	0.794(1)	1.001(4)	0.363(6)	0.002(7)	18
D1a	0.924(1)	0.770(1)	0.844(5)	0.363(6)	0.003(9)	18
D2b	1.048(1)	0.817(1)	1.007(4)	0.363(6)	0.006(8)	18
D2a	0.979(1)	0.770(1)	1.128(4)	0.363(6)	0.002(8)	18
D3a	0.975(2)	0.861(2)	0.647(8)	0.363(6)	0.08(2)	18
D3b	1.004(2)	0.816(2)	0.556(7)	0.363(6)	0.09(2)	18
D3c	1.046(2)	0.874(2)	0.728(8)	0.363(6)	0.10(2)	18
C13	1.000(3)	0.841(3)	0.681(8)	0.363(6)	0.07(2)	18

Table S22 Crystallographic data for activated Mn₂(dobdc), space group R-3, $a = 26.331(2)$ Å, $c = 7.0472(5)$ Å, $V = 4231.4(5)$ Å³, goodness of fit parameters, $R_p = 0.0352$, $wR_p = 0.0420$, $\chi^2 = 0.8767$. Values in parentheses indicate one standard deviation in the refined value.

Atom	X	Y	Z	Occ	Uiso (Å ²)	Multiplicity
Mn	0.3858(8)	0.361(1)	0.143(3)	1.0	0.003(5)	18
O1	0.3278(6)	0.2935(6)	0.362(2)	1.0	0.016(4)	18
O2	0.2998(8)	0.2278(7)	0.592(2)	1.0	0.018(4)	18
O3	0.3553(7)	0.2751(7)	0.013(3)	1.0	0.021(5)	18
C1	0.3188(5)	0.2443(5)	0.421(2)	1.0	0.007(3)	18
C2	0.3289(5)	0.2060(5)	0.290(2)	1.0	0.007(3)	18
C3	0.3440(6)	0.2215(5)	0.088(1)	1.0	0.003(3)	18
C4	0.3521(5)	0.1844(6)	-0.014(2)	1.0	0.001(3)	18
H1	.3605(9)	0.1928(9)	-0.164(3)	1.0	0.008(6)	18

Table S23 Crystallographic data for Mn₂(dobdc) loaded with 0.5 C₂D₆ per Mn (II), space group R-3, $a = 26.333(2)$ Å, $c = 7.0293(6)$ Å, $V = 4221.3(6)$ Å³, goodness of fit parameters, $R_p = 0.0483$, $wR_p = 0.0400$, $\chi^2 = 1.199$. Values in parentheses indicate one standard deviation in the refined value.

Atom	X	Y	Z	Occ	Uiso (Å ²)	Multiplicity
Mn	0.388(1)	0.356(2)	0.148(5)	1.0	0.02(1)	18
O1	0.327(1)	0.294(1)	0.369(4)	1.0	0.032(7)	18
O2	0.2990(9)	0.2263(9)	0.589(3)	1.0	0.028(6)	18
O3	0.355(1)	0.277(1)	0.019(3)	1.0	0.026(6)	18
C1	0.3167(8)	.2439(8)	0.425(3)	1.0	0.025(5)	18
C2	0.3267(7)	.2031(8)	0.291(2)	1.0	0.013(5)	18
C3	0.3432(8)	.2211(8)	0.083(2)	1.0	0.018(5)	18
C4	0.3520(8)	.1826(8)	0.023(3)	1.0	0.010(5)	18
H1	0.360(1)	0.195(1)	-0.166(5)	1.0	0.005(8)	18
C1a	0.526(2)	0.84612	0.654(5)	0.402(9)	0.01(1)	18
C1b	0.521(2)	0.861(2)	0.845(6)	0.402(9)	0.01(1)	18
D3	0.492(2)	0.802(2)	0.609(6)	0.402(9)	0.02(2)	18
D4	0.523(2)	0.878(2)	0.561(7)	0.402(9)	0.05(2)	18
D5	0.569(2)	0.851(2)	0.636(6)	0.402(9)	0.02(2)	18
D6	0.550(2)	0.902(2)	0.901(7)	0.402(9)	0.03(2)	18
D7	0.477(2)	0.856(2)	0.869(7)	0.402(9)	0.02(2)	18
D8	0.514(2)	0.828(2)	0.932(7)	0.402(9)	0.02(2)	18
C2a	0.33333	.66666	0.55(6)	0.25(1)	0.2(2)	18
Da	0.322(8)	.699(7)	.52(3)	0.25(1)	0.20(6)	18

Table S24 Crystallographic data for Mn₂(dobdc) loaded with 0.5 C₂D₄ per Mn(II), $a = 26.289(1)$ Å, $c = 7.0919(4)$ Å, $V = 4244.8(4)$ Å³, goodness of fit parameters, $R_p = 0.0283$, $wR_p = 0.0346$, $\chi^2 = 0.9663$. Values in parentheses indicate one standard deviation in the refined value.

Atom	X	Y	Z	Occ	Uiso (Å ²)	Multiplicity
Mn	0.3850(9)	0.358(1)	0.140(3)	1.0	0.017(6)	18
O1	0.3221(7)	0.2929(6)	0.353(2)	1.0	0.028(4)	18
O2	0.3016(6)	0.2299(6)	0.584(2)	1.0	0.020(4)	18
O3	0.3541(6)	0.2737(7)	0.014(2)	1.0	0.026(4)	18
C1	0.3180(5)	0.2450(5)	0.414(2)	1.0	0.019(4)	18
C2	0.3279(6)	0.2061(6)	0.286(2)	1.0	0.030(4)	18
C3	0.3435(8)	0.2218(7)	0.087(2)	1.0	0.029(4)	18
C4	0.3519(5)	0.1833(5)	-0.020(2)	1.0	0.008(3)	18
H1	0.3612(9)	0.1906(8)	-0.157(3)	1.0	0.011(6)	18
C11	0.963(1)	0.796(1)	0.882(4)	0.540(9)	0.029(8)	18
C12	1.002(1)	0.801(1)	1.026(5)	0.540(9)	0.06(1)	18
D1a	0.918(1)	0.768(1)	0.900(4)	0.540(9)	0.042(9)	18
D2b	1.047(1)	0.824(1)	1.009(4)	0.540(9)	0.039(9)	18
D2a	0.986(1)	0.7801(1)	1.154(5)	0.540(9)	0.04(1)	18
D1b	0.981(1)	0.8154(1)	0.744(3)	0.540(9)	0.06(1)	18

Table S25 Crystallographic data for Mn₂(dobdc) loaded with 0.25 C₃D₆ per Mn(II), $a = 26.309(2)$ Å, $c = 7.0668(5)$ Å, $V = 4236.0(5)$ Å³, goodness of fit parameters, $R_p = 0.0291$, $wR_p = 0.0353$, $\chi^2 = 0.9574$. Values in parentheses indicate one standard deviation in the refined value.

Atom	X	Y	Z	Occ	Uiso (Å ²)	Multiplicity
Mn	0.386(1)	0.360(1)	0.141(4)	1.0	0.010(8)	18
O1	0.3268(7)	0.2953(7)	0.355(2)	1.0	0.009(5)	18
O2	0.2996(8)	0.2257(8)	0.586(2)	1.0	0.009(4)	18
O3	0.3564(7)	0.2743(9)	0.006(3)	1.0	0.015(5)	18
C1	0.3182(7)	0.2452(7)	0.415(2)	1.0	0.024(5)	18
C2	0.3269(6)	0.2069(6)	0.288(2)	1.0	0.008(4)	18
C3	0.3431(7)	0.2224(7)	0.088(2)	1.0	0.009(4)	18
C4	0.3514(6)	0.1834(7)	-0.017(2)	1.0	0.004(4)	18
H	0.358(1)	0.189(1)	-0.162(4)	1.0	0.020(8)	18
C11	0.966(4)	0.799(4)	0.873(14)	0.224(6)	0.05(3)	18
C12	1.002(4)	0.804(3)	1.02(1)	0.224(6)	0.04(3)	18
D1a	0.922(3)	0.769(3)	0.88(1)	0.224(6)	0.02(2)	18
D2b	1.048(3)	0.820(3)	0.10(1)	0.224(6)	0.03(3)	18
D2a	0.985 (3)	0.781(3)	1.140(9)	0.224(6)	0.01(2)	18
D3a	1.034(4)	0.847(4)	0.69(1)	0.224(6)	0.05(3)	18
D3b	0.984(4)	0.868(3)	0.68(1)	0.224(6)	.05(2)	18
D3c	0.975(4)	0.806(4)	0.57(1)	0.224(6)	0.03(3)	18
C13	0.992(7)	0.830(7)	0.69(2)	0.224(6)	0.16(9)	18

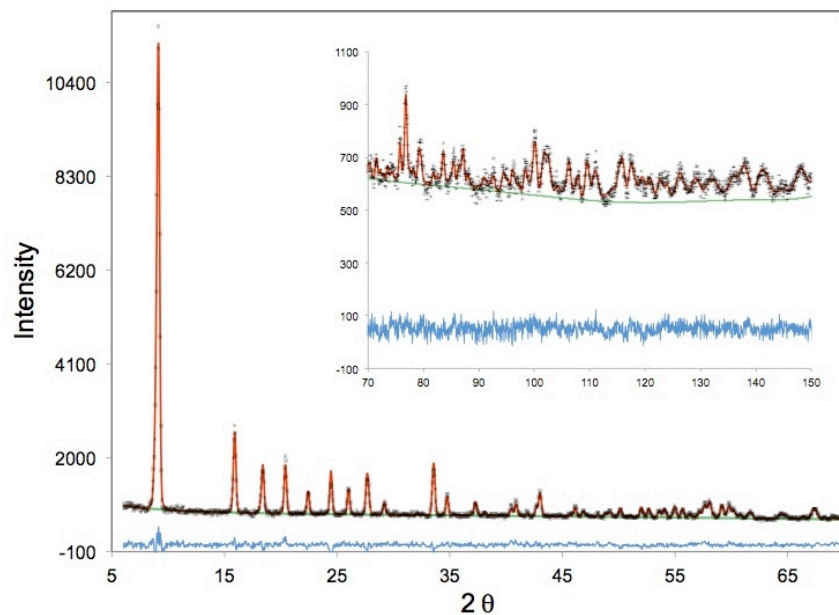


Fig. S8 Rietveld refinement of neutron powder diffraction data for desolvated $\text{Co}_2(\text{dobdc})$ at 10 K. Green lines, crosses, and red lines represent the background, experimental, and calculated diffraction patterns, respectively. The blue line represents the difference between experimental and calculated patterns. The final Rietveld fit parameter was $\chi^2 = 1.029$.

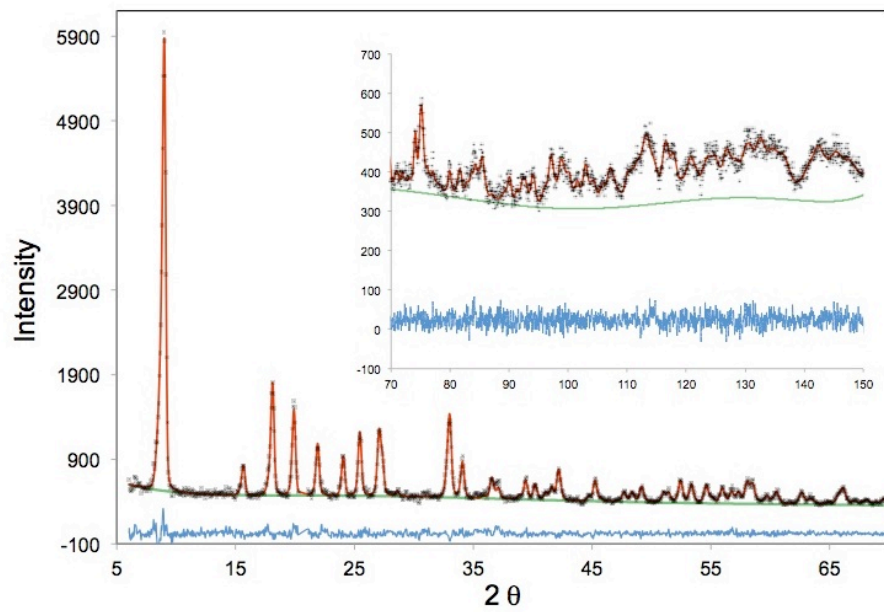


Fig. S9 Rietveld refinement of neutron powder diffraction data for desolvated $\text{Mn}_2(\text{dobdc})$ at 10 K. Green lines, crosses, and red lines represent the background, experimental, and calculated diffraction patterns, respectively. The blue line represents the difference between experimental and calculated patterns. The final Rietveld fit parameter was $\chi^2 = 0.8767$.

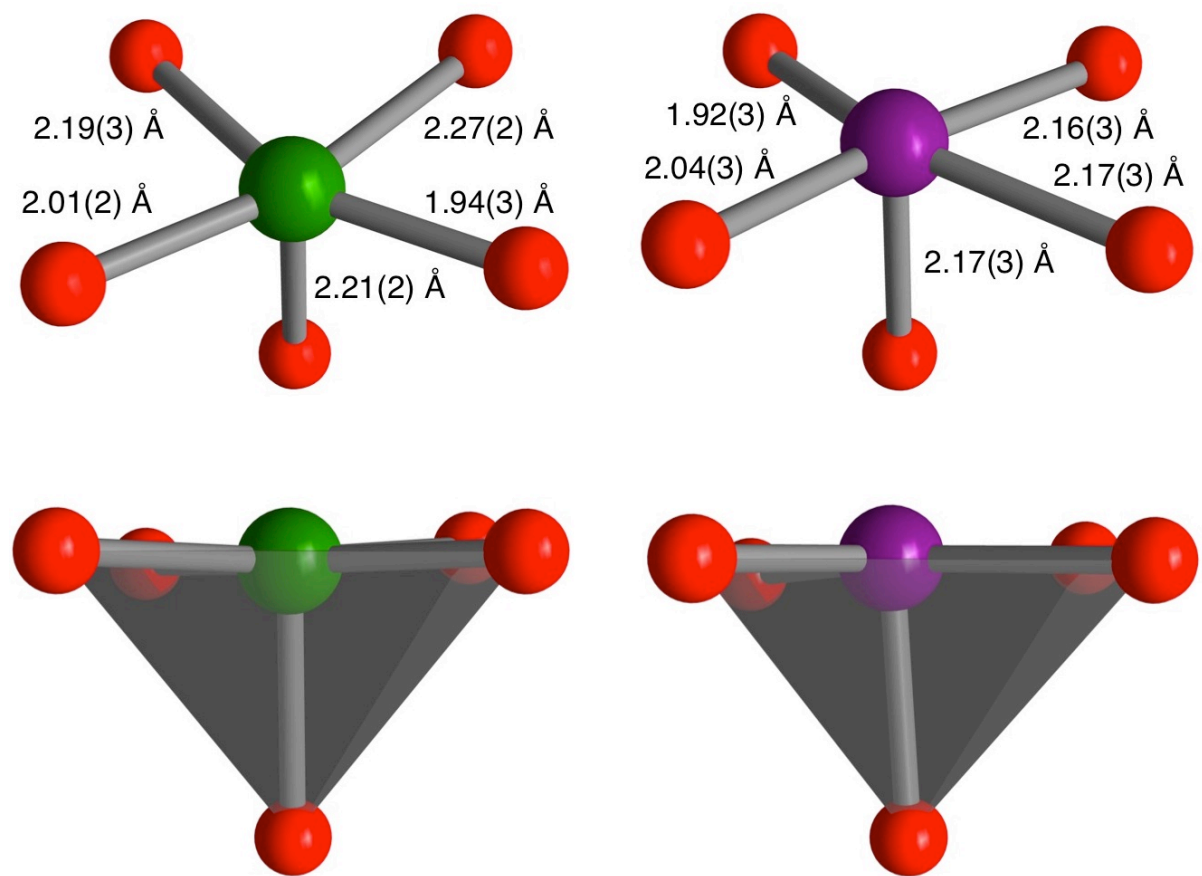


Fig. S10 Comparison of the coordination geometry at the square pyramidal metal cation in Mn₂(dobdc) (left) and Co₂(dobdc) (right). Values in parentheses indicate one standard deviation in the refined value.

9. Comparison to Prior Studies

Tables S26 and S27 compare hydrocarbon uptakes by M₂(dobdc) at 1 bar as measured in this study to those previously reported. Fig. S9 compares the adsorption of propane and propylene at 25 °C in a sample of Mn₂(dobdc) exhibiting a Langmuir surface area of 1284 m²/g to our data,⁸ collected at 45 °C using a sample of Mn₂(dobdc) with a Langmuir surface of 1797 m²/g.

Table S26 Ethane and ethylene uptakes at 1 bar in M₂(dobdc) from this work and previously reported isotherm data.

Gas	M ₂ (dobdc)	Reference	Temperature (K)	Uptake (mmol/g)
Ethane	Co	6	298	6.37
Ethane	Ni	6	298	5.39
Ethane	Zn	6	298	5.72
Ethane	Mg	7	318	5.15
Ethane	Co	8	298	6.41
Ethane	Mg	9	296	6.49
Ethane	Co	9	296	6.55
Ethane	Mg	This work	318	5.87
Ethane	Mn	This work	318	5.10
Ethane	Fe	4	318	5.10
Ethane	Co	This work	318	5.25
Ethane	Ni	This work	318	4.70
Ethane	Zn	This work	318	4.60
Ethylene	Co	6	298	6.93
Ethylene	Ni	6	298	7.96
Ethylene	Zn	6	298	6.37
Ethylene	Mg	7	318	6.64
Ethylene	Co	8	298	6.95
Ethylene	Mg	9	296	7.44
Ethylene	Co	9	296	7.00
Ethylene	Mg	This work	318	6.21
Ethylene	Mn	This work	318	6.30
Ethylene	Fe	4	318	6.28
Ethylene	Co	This work	318	6.05
Ethylene	Ni	This work	318	5.99
Ethylene	Zn	This work	318	5.36

Table S27 Propane and Propylene uptakes at 1 bar in M₂(dobdc) from this work and previously reported isotherm data.

Gas	M ₂ (dobdc)	Reference	Temperature (K)	Uptake (mmol/g)
Propane	Mg	7	318	6.60
Propane	Mg	8	298	4.66
Propane	Mn	8	298	4.67
Propane	Co	8	298	5.40
Propane	Mg	9	296	7.24
Propane	Co	9	296	5.22
Propane	Mg	This work	318	6.00
Propane	Mn	This work	318	5.68
Propane	Fe	4	318	6.12
Propane	Co	This work	318	5.90
Propane	Ni	This work	318	5.66
Propane	Zn	This work	318	5.46
Propylene	Mg	7	318	7.93
Propylene	Mg	8	298	5.95
Propylene	Mn	8	298	6.15
Propylene	Co	8	298	7.31
Propylene	Mg	9	296	8.45
Propylene	Co	9	296	6.14
Propylene	Mg	This work	318	7.46
Propylene	Mn	This work	318	7.21
Propylene	Fe	4	318	6.88
Propylene	Co	This work	318	6.82
Propylene	Ni	This work	318	6.94
Propylene	Zn	This work	318	6.29

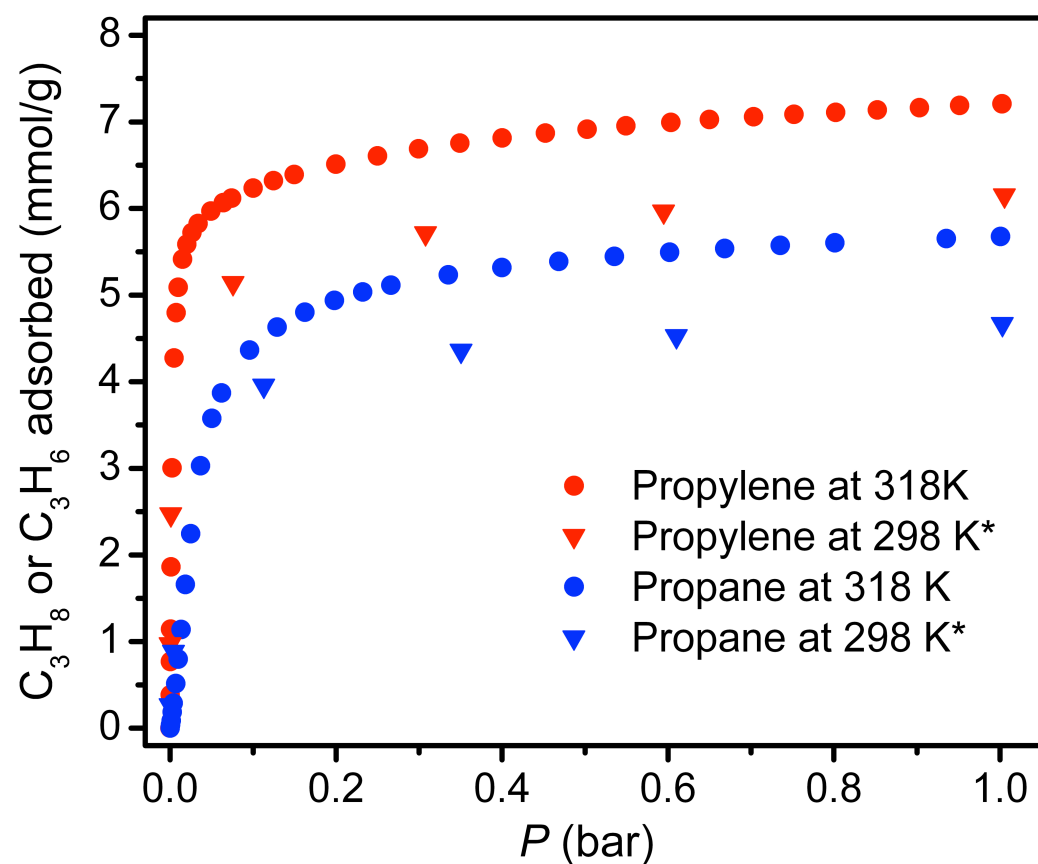


Fig. S11 Propane adsorption in $Mn_2(dobdc)$ at 25 °C from Snurr and coworkers (Langmuir surface area of $1284\text{ m}^2/\text{g}$) is compared to that measured in this work at 45 °C (Langmuir surface area of $1797\text{ m}^2/\text{g}$).

10. References

- 1 S. R. Caskey, A. G. Wong-Foy and A. J. Matzger, *J. Am. Chem. Soc.*, 2008, **130**, 10870-10871.
- 2 E. D. Bloch, L. J. Murray, W. L. Queen, S. Chavan, S. N. Maximoff, J. P. Bigi, R. Krishna, V. K. Peterson, F. Grandjean, G. J. Long, B. Smit, S. Bordiga, C. M. Brown and J. R. Long, *J. Am. Chem. Soc.*, 2011, **133**, 14814-14822.
- 3 E. Lemmon, M. McLinden and D. Friend, *Thermophysical Properties of Fluid Systems in NIST Chemistry Web Book*, eds. PJ Linstrom and WG Mallard, *NIST Standard Reference Database No. 69*, National Institute of Standards and Technology, Gaithersburg MD, 2010.
- 4 E. D. Bloch, W. L. Queen, R. Krishna, J. M. Zadrozny, C. M. Brown and J. R. Long, *Science*, 2012, **335**, 1606-1610.
- 5 A. L. Myers and J. M. Prausnitz, *AIChE J.*, 1965, **11**, 121-127.
- 6 A. J. Matzger, A. G. Wong-Foy and S. Caskey, *U.S. Pat.*, US 2010/0258004, **A1**, 2010.
- 7 Z. B. Bao, S. Alnemrat, L. Yu, I. Vasiliev, Q. L. Ren, X. Y. Lu and S. G. Deng, *Langmuir*, 2011, **27**, 13554-13562.
- 8 Y. S. Bae, C. Y. Lee, K. C. Kim, O. K. Farha, P. Nickias, J. T. Hupp, S. T. Nguyen and R. Q. Snurr, *Angew. Chem. Int. Ed.*, 2012, **51**, 1857-1860.
- 9 Y. He, R. Krishna and B. Chen, *Energy Env. Sci.*, 2012, **5**, 9107-9120.
- 10 B. H. Toby, *J. Appl. Cryst.*, 2001, **34**, 210-213.